

Investigation of the influence of workpiece-side parameters on the layer formation of zinc-coated boron-manganese steel

Franz He^{1, a *} and Marion Merklein^{1, b}

¹Lehrstuhl für Fertigungstechnologie, Friedrich-Alexander Universität Erlangen-Nürnberg,
Egerlandstr. 13, 91058 Erlangen, Germany

^afranz.he@fau.de, ^bmarion.merklein@fau.de

Keywords: Hot Stamping, Coating, 20MnB8

Abstract. The hot stamping process has been established as a technology for the production of ultrahigh-strength steel parts for safety-relevant components in lightweight construction for the automotive sector. Thanks to the reduced overall thickness combined with high tensile strength, it is possible to realize lightweight design concepts with improved crash behavior. Boron-manganese steels are usually used for this purpose. Due to initial process temperatures above 800 °C, hot stamping is considered a lubricant-free process. In addition to high friction and wear in the process, surface scaling and the need for tool repairs are the result. In light of these phenomena, hot stamping materials are coated to protect them from corrosion. Until now, aluminum-silicon-based coatings have been primarily used for the direct hot stamping route. While zinc-based coatings have so far mainly found usage in the indirect process route, they are now also become a valid alternative for the direct process route. In previous investigations, a significant influence of workpiece-side parameters on the formation of the coating during the austenitization process was found for aluminum-silicon (AlSi) coatings. In light of this, a similarly significant influence is suspected for zinc-based coatings. The parameters heating rate, furnace temperature and dwell time in the furnace and the effect on the coating formation of zinc-coated 20MnB8 during austenitization will be investigated. The resulting findings will form the basis for further experiments to investigate the influence of the parameters on friction and wear in the industry near strip drawing tests.

Introduction

Ever since the oil crisis in 1970 and the resulting shortage of raw materials, the demand for lighter and more energy-efficient automotive vehicles has increased, which has resulted in the increased use of ultra-high-strength steels [1]. In this regard, cold forming faces challenges due to springback, tool wear, and high forces in the process during the production of geometrically complicated components [1]. Forming at high temperatures allows an improvement of the formability with simultaneously reduced forces in the process as well as a higher dimensional stability [2]. For this purpose, the hot stamping process has been developed, which is based on a process combination of hot forming of fully austenitized blanks and hardening of the semi-finished product in the die within one process step [3]. Due to the martensitic microstructural transformation in the quenching process, the manufactured components achieve tensile strengths of up to 1500 MPa, which allows for improved crash properties with simultaneously reduced component weight [4]. Nowadays, hot-stamped components are used in impact beams, bumpers and side members [5]. Due to process temperatures above 850 °C necessary to achieve full austenitization in the steel material, lubricants are not stable during hot stamping. High friction and wear are the result which are significantly influenced by the process parameters [6]. Two process routes are available for hot stamping, the direct and indirect variants [7]. For both variants, the established boron-manganese steel 22MnB5 is widely in use [8]. In its initial state, this steel has a ferritic-pearlitic microstructure with a tensile strength of 500 to 700 MPa and an elongation



at break of over 10% [9]. When heated above the material-specific A_{c3} temperature of 850 °C, a complete transformation of the initial microstructure to austenite takes place [10]. The resulting reduction in strength and increase in elongation at break require low forces in the forming process and provide good conditions for the production of components with complicated geometries. Quenching above the critical cooling rate of 27 K/s results in martensite transformation, allowing improved mechanical properties to be obtained [4]. The boron-manganese steel can be used without an additional coating in the process, but a scale layer is formed during the austenitizing process due to the reaction with oxygen in the furnace atmosphere. The brittle and rough oxide layer impairs downstream process steps and results in a reduced heat transfer rate between the contact partners and thus reduced cooling rates [11]. Furthermore, the die surface is damaged by abrasive oxide particles, which is why the scale layer has to be removed by sand or shot blasting [12]. For this reason, semi-finished coatings are used for hot stamping to prevent the formation of an oxide layer. For direct hot stamping, aluminum-silicon (AlSi) based coatings are commonly used [10]. An unwanted material transfer of AlSi particles in the process leads to a deterioration of the tool surface, which results in a deviation from the dimensional accuracy of the component on the one hand, and different local heat transfer coefficients on the other hand, resulting in a reduction of the component quality [13]. Furthermore, the AlSi coating only provides a barrier effect and no cathodic protection [14], which limits its use in areas where electrolytic corrosion is of importance [1].

Zinc-based coatings have been mainly used for indirect hot stamping [3], where they exhibit a combination of high strengths in the base material while also providing a cathodic protection effect [5]. Due to the high risk of evaporation, run-off and oxidation of zinc coatings, due to the low melting temperature of 420 °C and evaporation temperature of 907 °C [3], the material was considered unsuitable for direct hot stamping [15]. This led to liquid metal-induced stress corrosion, where zinc diffuses into the material structure at high temperatures leading to material separation [2]. Due to recent developments the use of zinc-coated boron-manganese steel has also been made viable for direct hot stamping. By adding oxygen affine elements such as aluminum, a protective oxide skin (Al_2O_3) is formed on the component surface, which prevents oxidation of the zinc coating and inhibits the formation of a liquid phase by progressive formation of a higher-melting Zn-Fe layer [15]. In previous studies, the influence of process parameters during austenitizing on the layer formation of AlSi coatings was investigated. A significant influence of the furnace dwell time was found [16]. In light of these findings, the influence and interdependencies of process parameters on the coating formation are also investigated for the austenitization of zinc-coated boron manganese steels for direct hot stamping in order to determine significant parameters. The results of this work provide a data basis for further experiments to investigate the friction and wear behavior in the direct hot stamping process.

Methodology and experimental setup

Material and test procedure. Specimens with dimensions of 70 mm x 50 mm were used for the experiments. A 20MnB8 boron-manganese steel with a thickness of 1.5 mm coated with the ZF180 zinc coating was used as the test material. The coating was specially developed for the usage in direct hot stamping and prevents the formation of a liquid phase due to an intermediate precooling step [17]. This increases the time window required for cooling when using 22MnB5, consequently the required critical cooling rate of 27 K/s to reach martensite transformation cannot be achieved. The redistribution of alloying elements for the 20MnB8 base material shifts the ferrite, pearlite, and bainite regions, reducing the required cooling rate to 20 K/s [12] and ensuring a stable cooling corridor for martensite formation over a longer period [17]. The Gleeble 3500 GTC thermomechanical simulator from Dynamic Systems Inc. was used to study the influence of the heating rate. Here, the ends of the specimen are clamped in jaws through which an electric current flow is introduced. The resulting resistance causes local heating of the specimen [18]. The

temperature is monitored during the test run in the center of the specimen by welded-on type K thermocouples. Based on the findings during the investigation of the heating rate, further experiments on the furnace dwell time and temperature parameters were carried out in an ME87/13 annealing and hardening furnace from RHODE. The furnace can reach a maximum temperature of up to 1300 °C. A homogeneous furnace atmosphere and temperature distribution is ensured by three-sided chamber heating on the sides and bottom. A two-layer insulation structure reduces the power loss at the walls outside the furnace. The dimensions of the usable area in the furnace are 350 mm x 250 mm x 1000 mm [19].

Parameters and methodology. The parameters selected for the present study are based on the findings of past investigations done on AlSi coated 22MnB5. The heating rate, furnace temperature and dwell time for austenitization in the furnace were considered as critical influencing parameters [15]. The parameters were varied in three steps and repeated three times ($n=3$) to ensure reproducibility. The experiments were arranged based on the design of experiments and randomized for execution to prevent systematic errors. The exact parameters and variation levels can be found below in Table 1.

Table 1: Parameters and levels for the heating tests

Furnace temperature [°C]	880; 910
Furnace duration [s]	50; 125; 200
Heating rate [K/s]	5; 25; 50

After the test was carried out, the surface roughness R_z was recorded on the perthometer by means of tactile roughness measurement in accordance with DIN EN ISO 3274 and then cold-embedded, ground and polished for metallographic examination. The micrographs were analyzed for layer formation and layer height using a confocal light microscope, the Keyence VK-X200. In order to analyze the detected phase fractions, the elemental composition was also recorded using energy dispersive X-ray spectroscopy (EDS).

Results and discussion

Heat rate. The heating rate was investigated on a Gleeble 3500 GTC thermomechanical simulator. The heating rates were set at 5, 25 and 50 K/s. After reaching the target temperature of 910 °C, the specimen was held for 60 seconds and then cooled in air. The micrographs, shown in Fig. 1, show similar layer formation for all three heating rates. The base material of 20MnB8 can be found in the lower part of the image. The coating appears above the base material and separates into lighter and darker gray phases 1 and 2, followed by the embedding material.

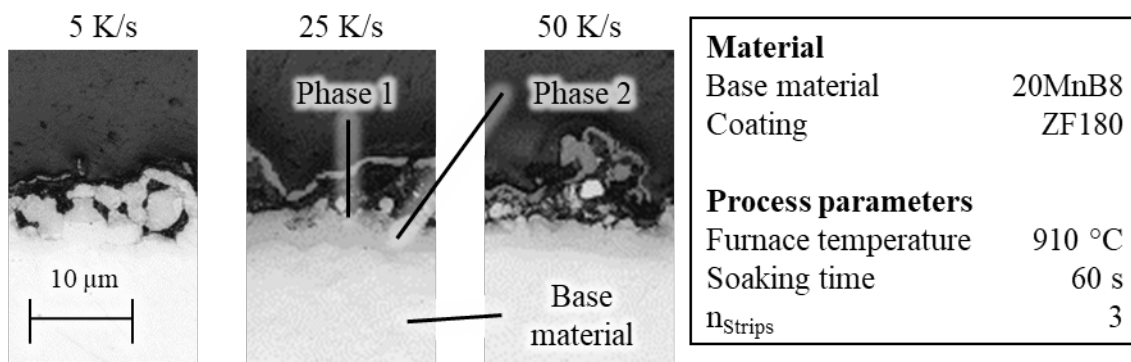


Fig. 1: Layer formation of the ZF180 coating at different heating rates

Based on the micrographs, no significant change in the coating formation due to the different heating rates can be detected. At heating rates >5 K/s, the test showed an increased susceptibility to reaction with impurities on the surfaces and a tendency for the coating to detach during the heating process, as shown in Fig. 2. The coating detachment can be attributed to an emergence of liquid zinc phases.

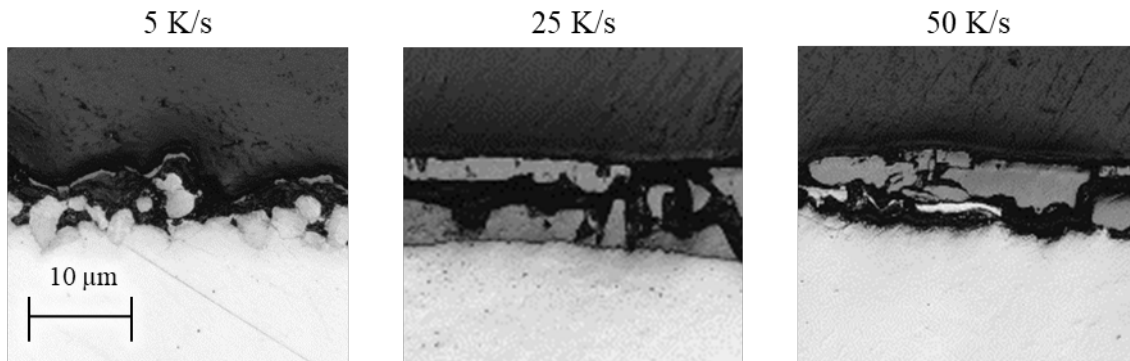


Fig. 2: Exemplary coating delamination due to liquid zinc phases at heating rates >5 K/s

The liquid zinc phases at heating rates >5 K/s occur due to the reduced time required to reach the target temperature. Melting of the zinc coating is inhibited by continuous diffusion of iron from the base material into the coating during the heating process, since the melting temperature of the Zn-Fe composition in the coating at 5 K/s is higher than the current furnace temperature. Since diffusion is a time-dependent parameter in addition to temperature, the phenomenon that not enough iron diffuses into the coating can occur at higher heating rates and the zinc phase exceeds its melting point. Due to the poor coating properties at higher heating rates and the non-significant influence on the coating formation, the influence of the heating rate will not be investigated further. Since the heating rate of the Gleeble shows a linear increase but conventional heating in roller furnaces, as used in the hot stamping industry, show a nonlinear temperature profile, further tests were carried out on an annealing and curing furnace. The heating rate at the furnace is 5 K/s and corresponds with the industrial standard.

Furnace temperature and dwell time. To investigate the influence of the furnace temperature, samples were heated to 880 °C and 910 °C. Furthermore, the duration in the furnace was varied between three dwell times (50 s, 125 s and 200 s) after reaching the furnace temperature. The specimens were placed on brackets in the furnace for the experimental procedure. This avoids direct contact with the furnace surface and altered heat conduction conditions, and ensures homogeneous heating by convection and thermal radiation through the furnace atmosphere. After the heat treatment, the samples were manually removed from the furnace and cooled down to ambient temperature in air. The surface roughness of the specimens was recorded after the heat treatment using perthometer measurements. The measurement of the surface roughness R_z can be found in Fig. 3. Additional tests with the same settings were carried out for the material 22MnB5 with the AlSi coating AS150 for comparison.

Compared to conventional 22MnB5 with AlSi coating, significantly higher roughness values are present for 20MnB8 with ZF180 coating. While no significant difference in roughness values can be seen for the parameter combinations with the AS150 coating, a significant difference in roughness R_z can be observed when the furnace temperature increases from 880 to 910 °C when using the ZF180 coating. The reason for this can be traced to the added alloyed elements aluminum and silicon which support the reaction with ambient oxygen in the furnace atmosphere. In the austenitizing process, these form a protective oxide skin (Al_2O_3) that prevents oxidation and melting of the zinc coating [15].

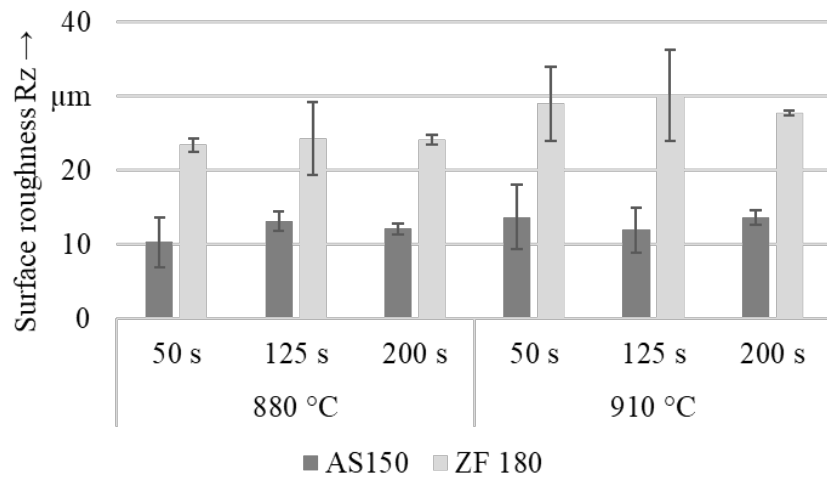


Fig. 3: Influence of the furnace duration and dwell time on surface roughness Rz

To further investigate the influence of the furnace parameters, micrographs of the samples were taken. With the help of EDS measurements, the occurring phase fractions were identified, these are shown for a dwell time of 50 s at a furnace temperature of 880 and 910 °C in Fig. 4. As already shown in Fig. 1, the same composition is visible with a ferritic base material followed by the coating and the embedding material. The coating splits into two phases, this occurs due to iron diffusion from the base material into the coating. This causes the formation of a zinc-rich gamma phase (Phase 1) with small amounts of iron, which occurs due to diffusion during galvanization of the material [5]. Phase 2 consists of an iron-rich zinc ferrite phase with a reduced zinc content compared to Phase 1 [12]. No traces of zinc elements can be found in the base material.

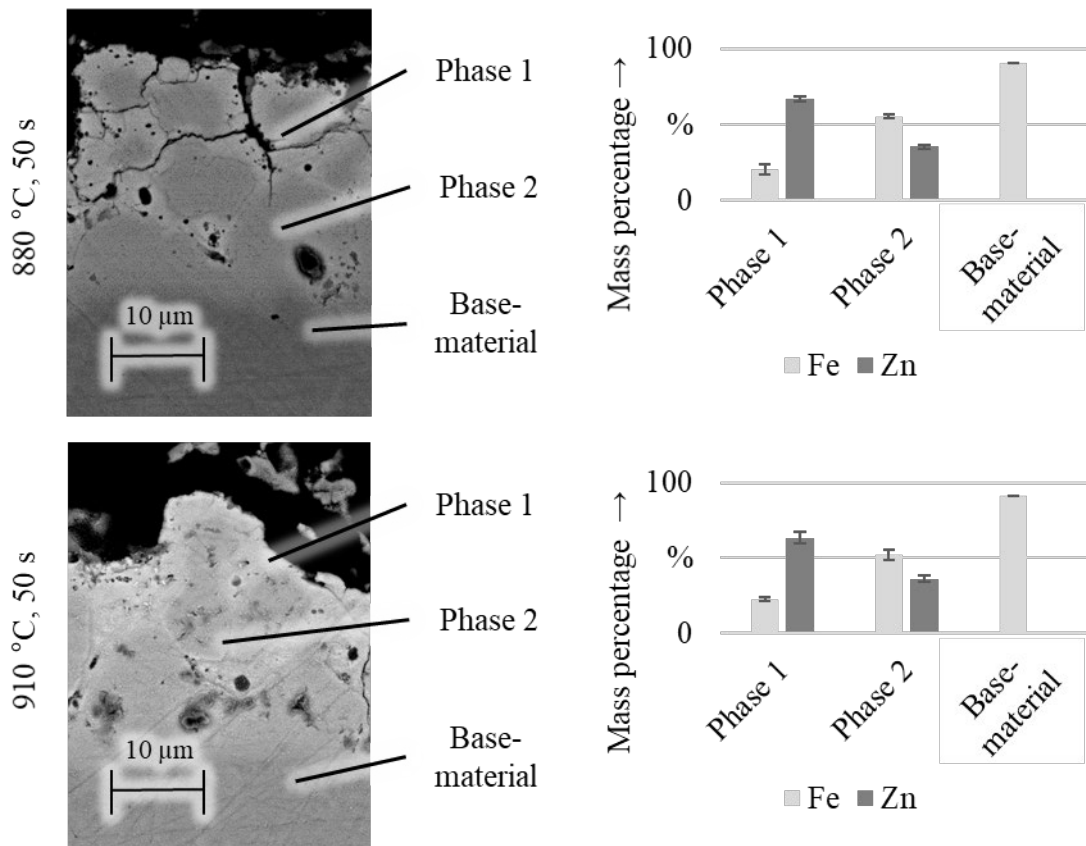


Fig. 4: EDS measurement of a ground section sample at a furnace temperature of 880 and 910 °C and dwell time of 50 seconds

With the further analysis of micrographs, it becomes clear that both an increase in the furnace temperature and the dwell time have a visible influence on the layer formation. An increase in furnace temperature from 880 to 910 °C results in a slight increase in the area fraction of Phase 2 and reduction of Phase 1. The same effect is more pronounced and better visible at a higher dwell time in the furnace for the sample. The composition of the phases however does not change significantly. The micrograph of samples held in the furnace at 880 and 910 °C for 300 seconds is shown in Fig. 5. The increase in Phase 2 at 880 °C is pronounced enough to almost completely displace Phase 1 due to the prolonged dwell time.

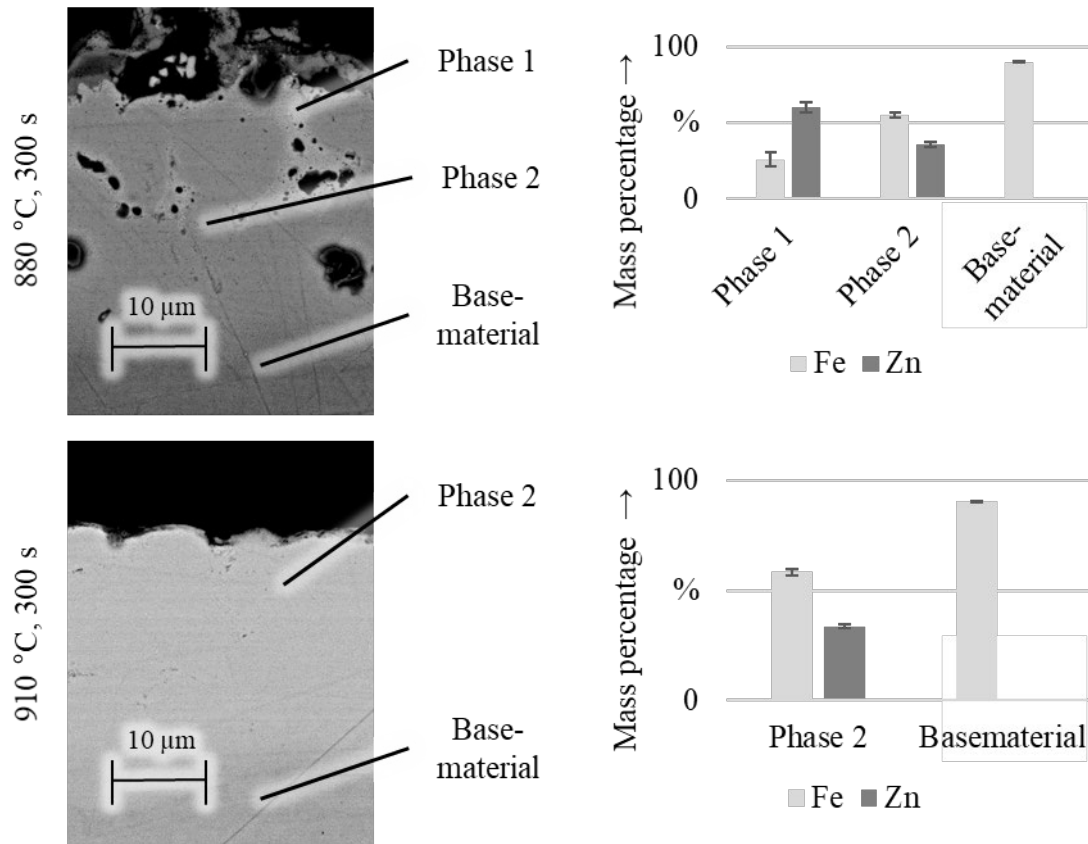


Fig. 5: EDX measurement of a ground sample at a furnace temperature of 880 and 910 °C and dwell time of 300 seconds

The lack of zinc elements in the base material suggests that no diffusion of zinc from the coating into the base material takes place within the parameter steps. Accordingly, the diffusion process occurs only one-way from the base material towards the coating. The process finds a saturation point at 910 °C and 300 seconds, where Phase 1 has completely turned into Phase 2 due to the ongoing diffusion process. The micrographs of samples with these parameter settings show no further zinc-rich gamma phase (Phase 1). These findings are in agreement with the results of Kondratiuk et al. [14] and Knezar et al. [15], who also conducted studies in the same subject area. A change in the height of the coating (Phase 1 and 2) could not be detected for any parameter combination due to the lack of zinc diffusion into the base material.

Summary and outlook

In this work, the layer formation of zinc-coated boron-manganese steel was analyzed under hot stamping conditions. The heating treatment parameters heating rate, furnace temperature and dwell time were varied and investigated with regard to their influence on the surface roughness Rz and layer formation in cross-sections. While a heating rate above 5 K/s does not cause any significant change in the coating components, it can still lead to flaking of the coating due to the formation of

a liquid zinc phase and thus cancel the corrosion protection. The furnace temperature has shown a significant effect on the surface roughness, while both furnace temperature and dwell time resulted in an increase of the iron-rich zinc phase and decrease of the zinc-rich gamma phase up to disappearance in the coating formation. The present work forms a basis for further investigations on the influence of heat treatment parameters on friction and wear in hot strip drawing tests for a realistic representation of the industrial hot stamping process. Furthermore, interactions with other relevant parameters with regard to friction and wear behavior should also be analyzed.

Acknowledgment

This study is part of the project P1291 “Workpiece-side Impact on the Tribological Conditions within Hot Stamping” funded by the Research Association for Steel Application (Forschungsvereinigung Stahlanwendung e.V. FOSTA). The authors would like to thank the Research Association for Steel Application for the financial support. Further thanks go to all cooperating industrial partners for their support and cooperation in this project.

References

- [1] Hardell J, Kassfeldt E and Prakash B, 2008 Friction and wear behaviour of high strength boron steel at elevated temperatures of up to 800°C *Wear* 9-10 788–99. <https://doi.org/10.1016/j.wear.2006.12.077>
- [2] Geiger M; Merklein M, 2007 Sheet Metal Forming - A New Kind of Forge for the Future *KEM* 9–20. <https://doi.org/10.4028/www.scientific.net/KEM.344.9>
- [3] Lechler J, Merklein M and Geiger M, 2006 Beschreibung des mechanischen Werkstoffverhaltens beim Warmumformen höchstfester Vergütungsstähle 1. Erlanger Workshop Warmblechumformung 1 13–30
- [4] Karbasian H; Tekkaya A E, 2010 A review on hot stamping *Journal of Materials Processing Technology* 15 2103–18. <https://doi.org/10.1016/j.jmatprotec.2010.07.019>
- [5] Autengruber R, Luckeneder G and Hassel A, W 2012 Corrosion of press-hardened galvanized steel *Corrosion Science* 12–19. <https://doi.org/10.1016/j.corsci.2012.04.048>
- [6] Venema J, Hazrati J, Matthews DTA, Stegeman R A and van den Boogaard A H, 2018 The effects of temperature on friction and wear mechanisms during direct press hardening of Al-Si coated ultra-high strength steel *Wear* 149–55. <https://doi.org/10.1016/j.wear.2018.04.006>
- [7] Bruschi S; Ghiotti A, 2014 Hot Stamping *Comprehensive materials processing* ed S. Hashmi (Amsterdam: Elsevier) pp 27–54. <https://doi.org/10.1016/B978-0-08-096532-1.00303-4>
- [8] Jüttner S, *Metallschutzgasschweißen von pressgehärteten höchstfesten Stählen mit unterschiedlichen Beschichtungskonzepten : Schlussbericht zu dem IGF-Vorhaben der Forschungsstelle(n) Otto-von-Guericke Universität Magdeburg/Institut für Werkstoff- und Fügetechnik (IWF): Otto von Guericke University Library, Magdeburg, Germany*
- [9] thyssenkrupp Issue: June 2020, version 0 MBW® Product information for manganese-boron steels for hot forming, Information on: https://www.thyssenkrupp-steel.com/media/content_1/publikationen/produktinformationen/mbw/thyssenkrupp_mbw_product_information_steel_en_10-2016.pdf [26.01.2022]
- [10] Dick P, Scheiker T and Mattes U, 2008 Warmumformung bei Daimler - Ein heiß diskutiertes Verfahren 3. Erlanger Workshop Warmblechumformung 41–55
- [11] Olah Neto A, Verran G O, Pissolatto G C and Dutra R R, 2016 Effect of Necking Behavior and of Gap Size on the Cooling Rate in Hot Stamping *Mat. Res.* 5 1138–43. <https://doi.org/10.1590/1980-5373-MR-2015-0654>

- [12] Kelsch R, Sommer A, Radlmayr K, Schwinghammer H, Faderl J, Kurz T, Luckeneder G, 2017 Hot Forming of Zinc Coated Press Hardening Steel. Characterization of Forming Behaviour and New Process Routes for Mass Production. *HOT SHEET METAL FORMING of HIGH-PERFORMANCE STEEL CHS²* ed M. Oldenburg, et al.) pp 337–344
- [13] Wang K, Gui Z, Liu P, Wang Y and Zhang Y, 2014 Cracking Behavior of Al-Si Coating on Hot Stamping Boron Steel Sheet *Procedia Engineering* 1713–18. <https://doi.org/10.1016/j.proeng.2014.10.218>
- [14] Kondratiuk J, Kuhn P, Labrenz E and Bischoff C, 2011 Zinc coatings for hot sheet metal forming: Comparison of phase evolution and microstructure during heat treatment *Surface and Coatings Technology* 17-18 4141–53. <https://doi.org/10.1016/j.surfcoat.2011.03.002>
- [15] K. Knezar, T. Manzenreiter, J. Faderl, K. M. Radlmayr K, 2007 Formhärten von feuerverzinktem 22MnB5: ein stabiler und reproduzierbarer Prozess 2. Erlanger Workshop Warmblechumformung ed M. Geiger, et al.(Bamberg: Meisenbach) pp 131–148
- [16] He F; Merklein M, 2021 Investigation of the impact of heat treatment on the layer formation of AlSi-coated boron-manganese steel *IOP Conf. Ser.: Mater. Sci. Eng.* 1 12009. <https://doi.org/10.1088/1757-899X/1157/1/012009>
- [17] Radlmayr K.; Kelsch R.; Sommer A.; Rouet C.; Kurz T.; Faderl J, *THE HOT FORMING OF GALVANIZED STEELS*, Information on: https://www.voestalpine.com/division_stahl/content/download/51623/646391/file/Whitepaper-The-hot-forming-of%20galvanized-steels-voestalpine.pdf [10.10.2022]
- [18] Gleeble® 3500-GTC System, Information on: <https://www.leeble.com/products/leeble-systems/leeble-3500.html> [06.10.2021]
- [19] Helmut RHODE GmbH: Technical Data Chamber Furnace ME 87/13, Information on: <https://www.rohde.eu/en/industry/products/chamber-furnaces/annealing-and-hardening-furnaces/me-87/13?c=146><https://www.rohde.eu/de/Pixelpdfdata/Articlepdf/id/81/onumber/IND-ME-87-13> [10.10.2022]